

Observation of the predissociated, quasilinear $\tilde{B}(^1A')$ state of CHF by optical-optical double resonance

Chong Tao and Scott A. Reid^{a),b)}*Department of Chemistry, Marquette University, Milwaukee, Wisconsin 53201*Timothy W. Schmidt and Scott H. Kable^{a),c)}*School of Chemistry, University of Sydney, NSW, 2006, Australia*

(Received 13 December 2006; accepted 16 January 2007; published online 7 February 2007)

We report the first observation of the predissociative \tilde{B} state of a halocarbene molecule. Rovibronic energy levels were measured in the $\tilde{B}(^1A')$ state of CHF by fluorescence dip detected optical-optical double resonance spectroscopy via the \tilde{A} state. The origin was found to lie 30 817.4 cm^{-1} above the zero point level of the \tilde{X} state. Rotational transitions within six purely bending states, and states involving one or two quanta of CF-stretch were observed, including the vibrational angular momentum components. Interpretation of the spectrum, with support of *ab initio* calculations, shows that CHF is quasilinear in the \tilde{B} state with a small (-200 cm^{-1}) barrier to linearity which lies below the zero-point level. The rotational constant, $B=1.04$ to 1.09 cm^{-1} , depending on vibrational state, again in good agreement with theory. All observed \tilde{B} state levels were predissociative, as evidenced by Lorentzian line broadening. Linewidths varied with initial state from 0.7–10.8 cm^{-1} , corresponding to excited state lifetimes of 0.5–8 ps. © 2007 American Institute of Physics.
[DOI: 10.1063/1.2515273]

I. INTRODUCTION

Carbenes are among the most important of reactive intermediates.¹ They are characterized by a divalent carbon giving rise to low-lying electronic states of different multiplicity, a singlet with two electrons paired in the “carbene” configuration, and a triplet biradical. Either of these configurations may be the ground state; the other is metastable. As common reaction intermediates these two states undergo different subsequent chemistry, e.g., as organic intermediates the carbene preserves reaction stereochemistry while the biradical does not.¹ Historically, therefore, much attention has focused on the singlet-triplet gap. The simplest carbene, methylene, has a well-known triplet ground state.² Most other small carbenes have singlet ground states, and have served as excellent benchmarks for theory.³ These systems are also prototypes for study of the Renner-Teller (RT) effect, as the two lowest singlet states are components of a RT pair, giving rise to an electronic spectrum in the visible region, readily probed by laser induced fluorescence (LIF). In recent years, the $\tilde{A} \leftrightarrow \tilde{X}$ systems of halocarbenes have been investigated extensively.^{3,4}

Despite the extensive literature on singlet-triplet gaps, RT interaction and $\tilde{A}-\tilde{X}$ spectroscopy, the ultraviolet photochemistry of carbenes is relatively unexplored apart from a couple of matrix studies.⁵ CFBr and CFCl are known to dissociate to CF+Br or Cl via a curve crossing in the \tilde{A} state.^{6,7} However this curve crossing seems not to be accessible in

the Franck-Condon region of most other small halocarbenes. There are very few investigations of higher lying electronic states. The ultraviolet (248 and 266 nm) photodissociation of CCl_2 has been explored recently, however, the identity of the dissociative surface remains uncertain.⁸ Even for the simplest carbene, CH_2 , weak transitions in the $\tilde{c}^1A_1 \leftarrow \tilde{a}^1A_1$ system observed some 60 years ago⁹ remained unassigned until very recently when rotationally resolved spectra of the \tilde{c} state were observed using optical-optical double resonance (OODR) spectroscopy.^{10–12} The energies accessed in the \tilde{c} state were just below the barrier to dissociation.

In this work, we report the first observation of the predissociative \tilde{B} state of a carbene, CHF, measured via a two color double resonance technique. As we shall demonstrate, this state is quasilinear with lifetime-broadened linewidths that vary with vibrational state. The equivalent one-photon transition is also allowed and would lie in the near ultraviolet ($\sim 310 \text{ nm}$) region. The \tilde{B} states of other carbenes are likely to behave in a similar manner and, therefore, this observation in CHF may represent a common photochemical mechanism for carbenes more generally.

II. EXPERIMENT

The apparatus used in this work is essentially the same as our previous CHF studies (at Marquette);¹³ only essential differences are highlighted. CHF was produced in a pulsed discharge nozzle through a 1–2% mixture of CH_2F_2 in Ar. Rotational transitions in the $\tilde{A} \leftarrow \tilde{X}(0_0^0)$ band of CHF were excited by a dye laser at $\sim 579 \text{ nm}$. About 300 ns later, a second counter-propagating laser either excited transitions in

^{a)} Authors to whom correspondence should be addressed.^{b)} Electronic mail: scott.reid@mu.edu^{c)} Electronic mail: s.kable@chem.usyd.edu.au

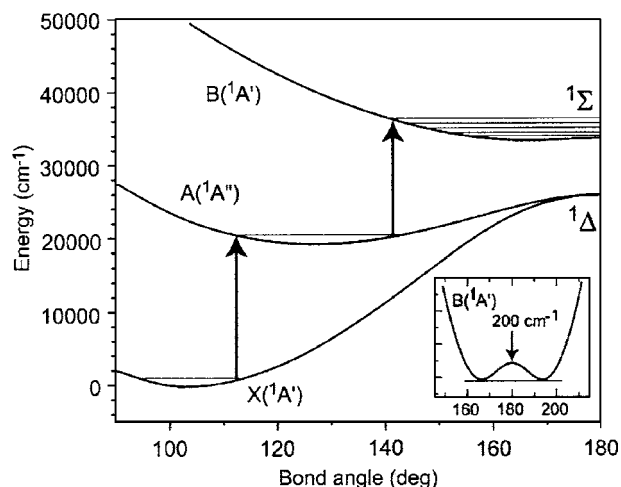


FIG. 1. *Ab initio* potential energy curves of the lowest three singlet states of CHF as a function of bond angle. The inset shows the \tilde{B} state on a scale to enhance observation of the barrier. The arrows indicate the experimental approach, which was to excite the $\tilde{A} \leftarrow \tilde{X}$ transition, then observe $\tilde{B} \leftarrow \tilde{A}$ transitions by depletion of the $\tilde{A} \rightarrow \tilde{X}$ fluorescence.

the $\tilde{B} \leftarrow \tilde{A}$ system or stimulated emission from $\tilde{A} \rightarrow \tilde{X}$ (see Fig. 1). A decrease in fluorescence was observed when the second laser was resonant with transitions in either $\tilde{B} \leftarrow \tilde{A}$ or $\tilde{A} \rightarrow \tilde{X}$ systems. Fluorescence depletion was measured using a dual gate boxcar system, where a portion of the fluorescence decay was integrated before and after the second laser pulse. The ratio of signal from each gate was recorded to remove the effect of shot-to-shot fluctuations in the signal. Typically, ten shots were averaged at each wavelength step.

The wavelength of the first laser was calibrated using the well-known $\tilde{X} \rightarrow \tilde{A}$ spectroscopic constants.¹³ The second laser was calibrated in part using stimulated emission pumping (SEP) transitions. Transitions terminating in $\tilde{X}(0,1,0)$, $(0,1,1)$, $(0,2,0)$, and $(1,0,0)$ were calibrated using published spectroscopic constants.¹⁴ Absolute frequency calibration of the $\tilde{A} \rightarrow \tilde{B}$ transitions, and hence \tilde{B} state term values is therefore accurate to ~ 0.5 cm^{-1} for spectra that contain these calibration lines. Other spectra were calibrated by interpolation and have an absolute calibration of approximately ± 2 cm^{-1} . Relative reproducibility within a spectrum should be accurate to ± 0.1 cm^{-1} which is the linewidth of the second laser.

III. RESULTS AND DISCUSSION

Figure 2 shows survey scans of $\tilde{B}(0, \nu_2, 0) \leftarrow \tilde{A}(0, 0, 0)$ bands with $\nu_2=0-5$. The x-axis is the two-photon energy above the \tilde{X} state zero-point energy. The bands display the characteristic rotational structure of a *c*-type, bent-to-linear transition, and our analysis follows closely that used in the recent report of the \tilde{B} state of SiH_2 using the same OODR technique.¹⁵ The selection rules for such a transition are $\Delta J = 0, \pm 1$, and $K_a - l = \pm 1$, where l is the vibrational angular momentum quantum number for the bending mode in the linear \tilde{B} state and K_a is the associated rotational quantum number of the bent molecule in the \tilde{A} state. There is an

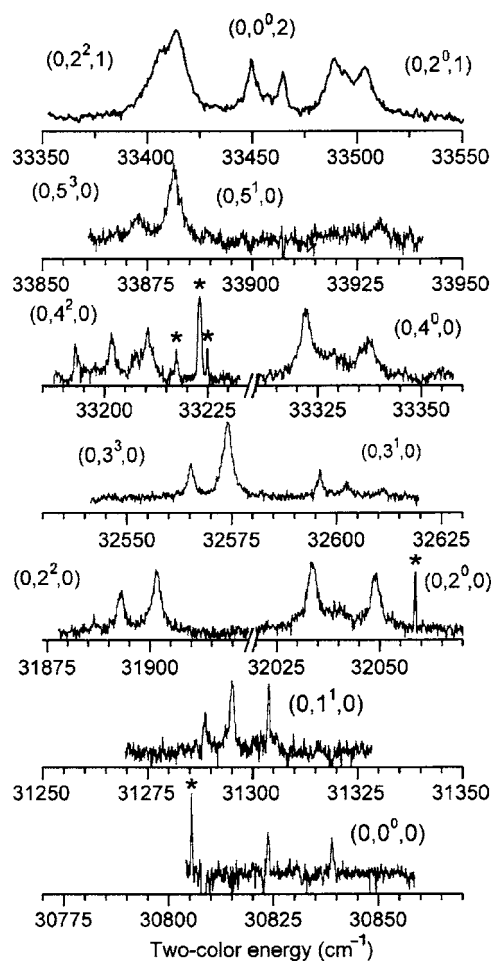


FIG. 2. Survey scans of the $\tilde{B} \leftarrow \tilde{A} \leftarrow \tilde{X}$ spectra of CHF. In each case, either the ${}^1R_0(2)$ band of the $\tilde{A} \leftarrow \tilde{X}$ transition was excited to probe \tilde{B} state levels with even ν_2 and $l=0$ or 2 , or the ${}^1R_1(2)$ transition to probe levels with $\nu_2 = \text{odd}$ and $l=1$ or 3 . The upper panel shows excitation of two vibrational bands involving the CF-stretch vibration. Note that the scale is 200 cm^{-1} , in order to fit these very broad bands onto the spectrum. Asterisks indicate $\tilde{A} \rightarrow \tilde{X}$ SEP transitions.

additional selection rule governing transitions between each K_c doublet in the \tilde{A} state with states of different parity in the \tilde{B} state. However, we do not resolve the K_c nor parity doublets in these experiments. By pumping intermediate \tilde{A} state levels with $K_a=0, 1$, and 2 , \tilde{B} state levels with $l=0-3$ could be accessed with the restriction that even ν contains only even l components and vice versa for odd ν . The lowest two vibrational states in Fig. 2 show only one l component, while all higher levels contain two l components. The only pure bending states of a linear molecule that contain only one l component are the two lowest lying states: $(0,0^0,0)$ and $(0,1^1,0)$. This provides convincing evidence that the band at $30\,817.4$ cm^{-1} is the \tilde{B} state origin.

Although the bands in Fig. 2 can be described in terms of bent to linear transitions, it remains to determine whether the equilibrium geometry of the \tilde{B} state is truly linear, or quasilinear. To establish the case we performed a simple test of quasilinearity¹⁶ and also calculated the potential energy along the bend coordinate at a diagnostic level of *ab initio* theory.

Yamada and Winnewisser define a quasilinearity parameter as:¹⁶

$$\gamma_0 = 1 - 4 \left(\frac{A}{\omega_{bend}} \right), \quad (1)$$

where A is the rotational constant about the a -axis and ω_{bend} the bending frequency. In the quasilinear case, this equation becomes:

$$\gamma_0 = 1 - 4 \left(\frac{\omega(0, 1^1, 0)}{\omega(0, 2^0, 0)} \right). \quad (2)$$

γ_0 will therefore vary between ≈ 1 for a bent molecule, to -1 for a linear molecule. To illustrate, $\gamma_0 = 0.95$ for \tilde{X} state CHF, near the limiting value for a bent molecule. $\gamma_0 = 0.90$ in the \tilde{A} state, clearly bent but with an increase in bond angle. In contrast, $\gamma_0 = -0.54$ in the \tilde{B} state, which is similar to the quasilinear \tilde{B} state of SiH₂ for which a small barrier at linearity of ~ 125 cm⁻¹ was inferred.¹⁵

To place the structure of the \tilde{B} state on a stronger theoretical footing, we performed a preliminary theoretical exploration of the electronic structure. The potential energy curves of the \tilde{X} , \tilde{A} , and \tilde{B} electronic states were computed using MOLPRO¹⁷ and the complete active space self-consistent-field (CASSCF) method.^{18,19} The active space used was complete valence, consisting of all 9 molecular orbitals which arise from the $2s$, $2p$ atomic orbitals of the C and F atoms, and the $1s$ orbital of the H atom, which accommodate the 12 active valence electrons. While the core orbitals were held closed, they were optimized in the CASSCF procedure. In calculating the \tilde{X} and \tilde{A} states, even weightings were given in the CASSCF orbital optimization in order to ensure degeneracy at linearity. The \tilde{B} state was calculated separately with full weighting given to that state. The basis set used was the correlation-consistent cc-pVTZ basis.²⁰ The HCF bond angle was scanned with R_{CH} and R_{CF} fixed at 1.06 Å and 1.29 Å, respectively, which were determined to be the equilibrium bond lengths for the \tilde{B} state at linearity. These calculations used the same basis set, but lower level of theory than we used previously for an extensive investigation of the \tilde{X} , \tilde{a} , and \tilde{A} states of CHF.²¹ The lower level of theory still provides \tilde{X} - \tilde{A} and \tilde{X} - \tilde{B} energies that are within 10% of the experimental values.

Figure 1 shows the resultant *ab initio* bending potential energy curves. The inset shows the \tilde{B} state alone, drawn with a scale to accentuate the barrier at linearity (~ 200 cm⁻¹). This is in good agreement with the interpretation based on the quasilinear parameter above. The rotational constant at the linear configuration was calculated to be $B = 1.081$ cm⁻¹, also in excellent agreement with the experimental value at the zero-point level (Table I). The calculated curve is consistent with the observed energy levels (Table I).

Figure 3 shows the $(0, 2^l, 0)$ transitions at higher resolution accessed via different \tilde{A} rotational levels: $J_{Ka} = 1_1, 2_1,$ and 3_1 . The effect of the double resonance technique is clear; each spectrum shows absorption from a single \tilde{A} state level. Excitation of several intermediate levels with different J al-

TABLE I. Assignments, energies, rotational constants and line widths of all \tilde{B} state vibrational levels measured in this work.

Vib. levels	Vib. Energy ^a (exp, cm ⁻¹)	B^b (exp, cm ⁻¹)	Width ^c (cm ⁻¹)
(0,0,0)	0.0	1.080±0.006	0.7
(0,1 ¹ ,0)	466.9	1.092±0.003	1.1
(0,2 ² ,0)	1069.1	1.079±0.008	2.4
(0,2 ⁰ ,0)	1209.8	1.078±0.010	3.1
(0,3 ³ ,0)	1748.0	1.082±0.005	2.2
(0,3 ¹ ,0)	1773.5	1.088±0.003	1.6
(0,4 ² ,0)	2378.1	1.067±0.010	2.0
(0,4 ⁰ ,0)	2498.7	1.050±0.010	4.0
(0,5 ³ ,0)	3055.4	1.079±0.010	3.1
(0,5 ¹ ,0)	3060.8	1.076±0.006	2.5
(0,0 ⁰ ,1)	1329.4	1.082±0.020	1.0
(0,1 ¹ ,1)	1896.1	1.075±0.007	6.9
(0,2 ² ,1)	2582.1	1.073±0.025	10.8
(0,2 ⁰ ,1)	2665.2	1.040±0.013	9.1
(0,0 ⁰ ,2)	2626.4	1.040±0.004	5.1

^aMeasured relative to the zero-point level which lies $30\,817.4 \pm 2.0$ cm⁻¹ above the zero-point level of the \tilde{X} state. The relative uncertainty in the vibrational energy is ± 0.5 cm⁻¹.

^bFit using a linear molecule rigid rotor to about 5 spectral lines.

^cFit to a Lorentzian line profile. These linewidths should be considered indicative. No tests for power broadening were performed, although SEP lines were always < 0.3 cm⁻¹.

lowed measurement of 3–5 rotational states in each vibrational level sufficient to determine approximate rotational constants, B , which are reported in Table I. All pure bending levels have $B = 1.08$ – 1.09 cm⁻¹, except for the $(0, 4^l, 0)$ levels. The $(0, 4^0, 0)$ level, in particular, is more substantially broadened than the other pure bending levels, indicating that it is probably perturbed by a nearby, shorter lived state.

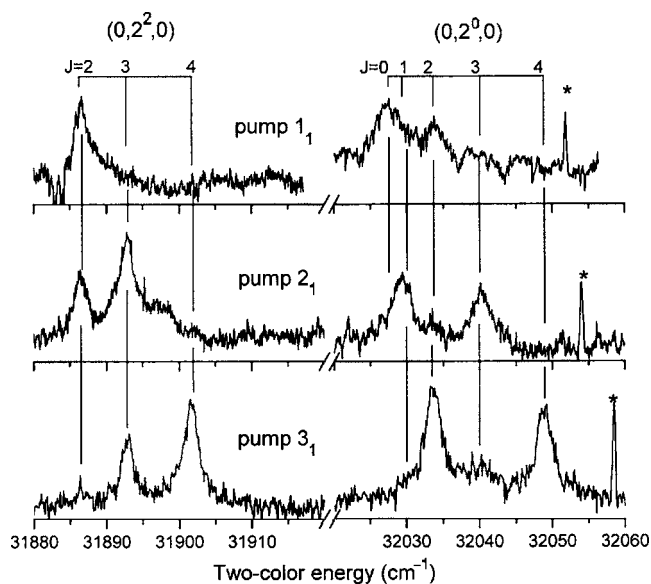


FIG. 3. Higher resolution scans of the $\tilde{B}(0, 2^l, 0) \leftarrow \tilde{A}(0, 0, 0)$ transition using different intermediate rotational states (indicated on the figure). Both l components are clear, and up to three rotational states for each l can be prepared via a single \tilde{A} state level. Asterisks indicate $\tilde{A} \rightarrow \tilde{X}$ SEP transitions.

In addition to the bending levels, several transitions to levels involving 1 or 2 quanta of C–F stretch: $(0, \nu', 1)$ and $(0, \nu', 2)$ were observed. Three such transitions terminating in $(0, 0^0, 2)$, $(0, 2^0, 1)$, and $(0, 2^2, 1)$ are shown in the top panel of Fig. 2. (Note the x -axis for this panel has twice the range of the other panels.) The peaks have Lorentzian linewidths of $\sim 10 \text{ cm}^{-1}$, corresponding to a transform-limited lifetime of $\sim 0.5 \text{ ps}$. These states lie near the $(0, 4^1, 0)$ levels and appear to be in Fermi resonance because the l -splitting appears anomalous in comparison to the other bending states; $(0, 4^0, 0)$ in particular appears to be perturbed by $(0, 2^0, 1)$. The CF-stretching levels all exhibit a smaller rotational constant, $B = 1.04\text{--}1.08 \text{ cm}^{-1}$, consistent with a slightly larger CF bond length in the excited vibrational states.

Lorentzian linewidths were fit for all measured $\tilde{B} \leftarrow \tilde{A}$ transitions. In every case these were broader than the SEP lines indicating that the upper levels are homogeneously broadened by predissociation (Table I) which is consistent with the fact that the \tilde{B} state origin lies some $6\,000 \text{ cm}^{-1}$ above the thermochemical threshold to form $\text{CF}(^2\Pi)$ and H products.²¹ However, the widths display a striking dependence on vibrational state, with CF-stretch-containing states exhibiting far larger widths than nearly isoenergetic $(0, \nu', 0)$ states. This suggests that studies of the \tilde{B} state dynamics will be of interest in understanding the state interactions important in the photochemistry of carbenes.

As noted earlier, the \tilde{B} state of CHF is the same electronic configuration as the \tilde{c} state of CH_2 .^{9–12} The \tilde{c} state of CH_2 lies below the thermochemical dissociation limit, while for CHF, the \tilde{B} state is clearly above. Other halocarbenes are likely to be similar to CHF and hence the \tilde{B} states in these other carbenes might also be photochemically active, as they should be one-photon-allowed by symmetry, though weak, because they involve a two-electron transition.

IV. CONCLUSIONS

We have reported the first observation of the predissociated \tilde{B} state of CHF using OODR spectroscopy. Transitions involving the bend and CF-stretch vibrations were identified. The linewidths display pronounced mode specificity with a significant increase observed upon excitation of CF-stretch levels. A preliminary vibrational analysis indicates that the upper state is quasilinear, consistent with our theoretical predictions, which predict a barrier height of $\sim 200 \text{ cm}^{-1}$.

ACKNOWLEDGMENTS

S.A.R. and S.H.K. acknowledge an Australian Academy of Science fellowship which allowed us to collaborate on this project. S.A.R. acknowledges the National Science Foundation (Grant No. CHE-0353596) for research support. S.H.K. and T.W.S. acknowledge the Australian Research Council for project funding (DP0665831). All authors thank Calvin Mukarakate and Yulia Mishchenko for experimental assistance and discussions regarding this work.

¹ See, e.g., *Reactive Intermediate Chemistry*, edited by R. A. Moss, M. S. Platz, and M. Jones, Jr., (Wiley-Interscience, Hoboken, NJ, 2004), Chaps. 7–9.

² See, e.g., G. Herzberg and J. Shoosmith, *Nature (London)* **183**, 1801 (1959); G. Herzberg, *Proc. R. Soc. London, Ser. A* **262**, 291 (1961).

³ See, e.g., H.-G. Yu, T. Lezana-Gonzalez, A. J. Marr, J. T. Muckerman, and T. J. Sears, *J. Chem. Phys.* **115**, 5433 (2001); C.-S. Lin, Y.-E. Chen, and B.-C. Chang, *J. Chem. Phys.* **121**, 4164 (2004); T. W. Schmidt, G. B. Bacskay, and S. H. Kable, *J. Chem. Phys.* **110**, 11277 (1999); C. Tao, C. Mukarakate, and S. A. Reid, *J. Chem. Phys.* **124**, 224314 (2006), and references therein.

⁴ See, e.g., T. Suzuki, S. Saito, and E. Hirota, *Can. J. Phys.* **62**, 1328 (1984); D. J. Clouthier and J. Karolczak, *J. Chem. Phys.* **94**, 1 (1991); B.-C. Chang and T. J. Sears, *J. Chem. Phys.* **102**, 6347 (1995); T.-C. Tsai, C.-W. Chen, and B.-C. Chang, *J. Chem. Phys.* **115**, 766 (2001); C. A. Richmond, J. S. Guss, K. Nauta, and S. H. Kable, *J. Mol. Spectrosc.* **220**, 137 (2003); M. Deselnicu, C. Tao, C. Mukarakate, and S. A. Reid, *J. Chem. Phys.* **124**, 134302 (2006), and references therein.

⁵ See, e.g., G. Maier and H. P. Reisenauer, *Adv. Carbene Chem.* **3**, 115 (2001); R. A. Seburg, E. V. Patterson, J. F. Stanton, and R. J. McMahon, *J. Am. Chem. Soc.* **119**, 5847 (1997).

⁶ J. S. Guss, O. Votava, and S. H. Kable, *J. Chem. Phys.* **115**, 11118 (2001).

⁷ P. T. Knepp, C. K. Scalley, G. B. Bacskay, and S. H. Kable, *J. Chem. Phys.* **109**, 2220 (1998); P. T. Knepp and S. H. Kable, *J. Chem. Phys.* **110**, 11789 (1999).

⁸ S. K. Shin and P. J. Dagdigian, *Phys. Chem. Chem. Phys.* **8**, 3446 (2006); *J. Chem. Phys.* **125**, 133317 (2006).

⁹ G. Herzberg and J. W. C. Johns, *Proc. R. Soc. London, Ser. A* **295**, 107 (1966).

¹⁰ Y. Kim, A. V. Komissarov, G. E. Hall, and T. J. Sears, *J. Chem. Phys.* **123**, 024306 (2005).

¹¹ Y. Kim, G. E. Hall, and T. J. Sears, *Phys. Chem. Chem. Phys.* **8**, 2823 (2006).

¹² Y. Kim, G. E. Hall, and T. J. Sears, *J. Mol. Spectrosc.* **240**, 269 (2006).

¹³ H. Fan, I. Ionescu, C. Annesley, J. Cummins, M. Bowers, J. Xin, and S. A. Reid, *J. Chem. Phys.* **108**, 3732 (2004).

¹⁴ T. Suzuki and E. Hirota, *J. Chem. Phys.* **85**, 5541 (1986).

¹⁵ Y. Muramoto, H. Ishikawa, and N. Mikami, *J. Chem. Phys.* **122**, 154302 (2005).

¹⁶ K. Yamada and M. Winnewisser, *Z. Naturforsch. A* **31A**, 139 (1976).

¹⁷ MOLPRO, version 2006.1. a package of *ab initio* programs, written by H.-J. Werner, P. J. Knowles, R. Lindh *et al.* see <http://www.molpro.net>.

¹⁸ B. O. Roos, P. R. Taylor, and P. E. S. Siegbahn, *Chem. Phys.* **48**, 157 (1980); B. O. Roos, *Ab initio Methods in Quantum Chemistry* (Wiley, Chichester, UK, 1987), Vol. II, p. 399.

¹⁹ H.-J. Werner and P. J. Knowles, *J. Chem. Phys.* **82**, 5053 (1985); P. J. Knowles and H.-J. Werner, *Chem. Phys. Lett.* **115**, 259 (1985).

²⁰ T. Dunning, Jr., *J. Chem. Phys.* **90**, 1007 (1989).

²¹ T. W. Schmidt, G. B. Bacskay, and S. H. Kable, *Chem. Phys. Lett.* **292**, 80 (1998).